SAND98-2534C

THE ELECTRICAL PROPERTIES OF NATIVE AND DEPOSITED THIN ALUMINUM OXIDE LAYERS ON ALUMINUM: HYDRATION EFFECTS

J. P. Sullivan, J. C. Barbour, R. G. Dunn, K.-A. Son, L. P. Montes, N. Missert, and R. G. Copeland
Sandia National Laboratories, Albuquerque, NM 87185

ABSTRACT

The electronic defect density of native, anodic, and synthetic Al oxide layers on Al were studied by solid state electrical measurement as a function of hydration of the oxide. The non-hydrated synthetic Al oxide layers, which included electron cyclotron resonance (ECR) plasma deposited oxides as well as ECR plasma grown oxides, were highly insulating with electrical transport dominated by thermal emission from deep traps within the oxide. Following hydration these oxides and the native oxides exhibited a large increase in electronic defect density as evidenced by increases in the DC leakage current, reduction in the breakdown field, and increase in AC conductance. Elastic recoil detection of hydrogen revealed that hydration leads to hydrogen incorporation in the oxide films and hydrogen injection through the films into the Al layer below. The increase in electronic defect concentration is related to this hydrogenation and may play a significant role in localized corrosion initiation.

INTRODUCTION

Aluminum owes its corrosion resistance to a thin passivating layer of aluminum oxide (1). For sufficiently aggressive environments or at sufficiently high anodic potentials, this passivation layer is locally compromised, and a corrosion site, i.e. a pit, forms. The mechanism by which this localized electrochemical attack initiates is presently unknown. It is expected, however, that defects (whether chemical, structural, or electronic in nature) that are present within the passivation layer may be the deterministic factor for the spatial localization (2). It is the objective of this investigation to assess the defect structure of native, anodic, and synthetic, e.g. deposited, Al oxides on Al through the use of electrical measurements. The study of synthetic Al oxides on Al is of interest because, in this system, the defect structure of the Al oxide can be controlled independently of the intrinsic defects present in the metal, e.g. grain boundaries, second phase particles, etc. This permits de-coupling of the electrochemical influence of oxide defects from the electrochemical influence of metallurgical defects. Another key aspect of this research effort was to develop understanding of the modifications which occur in anhydrous aluminum oxide layers following hydration. This is a fundamental first step in the electrochemical analysis of Al oxide/Al.

EXPERIMENTAL

The samples used in this study were generated by electron beam evaporation of Al, within a vacuum chamber (base pressure of ~ 10^{-9} Torr), at a rate of 1 Å/sec. on to a

DISCLAIMER

substrate at room temperature. The substrate consisted of a 2 μm thick SiO_2 layer (either thermally-grown or chemical-vapor-deposited and annealed at 1100°C) on Si. The SiO_2 layer provided electrical isolation between the deposited Al and underlying Si. The Al films formed in this manner were polycrystalline with a random grain orientation and average grain size of 0.15 μm. Typical Al film thicknesses were 0.15-0.2 μm.

Aluminum oxide layers were formed on these Al films by several methods: 1. air exposure (defined as 90 min. exposure to 1 Torr O_2(g) immediately after Al film growth, followed by exposure to a room ambient environment), 2. anodic oxidation, 3. electron cyclotron resonance (ECR) plasma oxide deposition, or 4. ECR plasma oxide growth. The anodic oxidation was performed by anodically polarizing the Al samples at voltages of 3.57 V and 7.14 V with respect to open circuit potential in a solution of 0.5 M H_3BO_3 – 0.05 M $Na_2B_4O_7$. These voltages were chosen to create anodic aluminum oxide layers of approximately 50 Å and 100 Å in thickness, respectively (3). The ECR plasma-deposited alumina layers were created by simultaneous Al evaporation in the presence of an oxygen plasma. This approach has been shown to yield highly controllable (in stoichiometry, composition, and crystallinity) alumina layers which are dense (non-porous) and free of macro-defects, e.g. pinholes (4). The typical deposited alumina layers used in this study were 200 Å thick, stoichiometric, and amorphous in structure. The ECR grown oxides were synthesized by exposure of a freshly-deposited Al layer to an ECR O_2 plasma for times ranging from 10 min. to several hours. The oxides produced in this manner ranged in thickness from 30 Å to 50 Å.

Samples for electrical measurement were prepared by photolithographically patterning Au contacts with areas ranging from ~ 2 x 10^{-7} cm^2 to 4 x 10^{-4} cm^2. The most frequently used contact size was 2.5 x 10^{-5} cm^2 in area (a square contact 50 μm by 50 μm). The Au layer was electron beam deposited under high vacuum on to samples having patterned photoresist on their surfaces, and lift-off was used to create the contacts. The electrical characterization was performed on capacitor (metal-insulator-metal) structures using the Au top contact as one electrode and the Al layer beneath the oxide as the bottom electrode. The DC electrical measurements included current-voltage sweeps (between ~ -1 V to +1 V) followed by sweeps to higher potentials (typically a few volts either positive or negative) until dielectric breakdown occurred. Measurements were performed at room temperature with a sweep rate of approximately 10 mV/sec. and an instrumental noise level of 10 fA. The AC electrical measurements included capacitance-frequency and AC conductance-frequency sweeps over the frequency range of 1 Hz to 1 MHz. The frequency sweep was completed in approximately 10 minutes.

X-ray reflectivity measurements of oxide layer thickness and density were performed on the same samples used for electrical measurement, in areas adjacent to the electrical tests. The stoichiometry (O/Al ratio) of the thicker oxide films was obtained using 2.8 MeV He^+ Rutherford Backscattering spectrometry (RBS) at a scattering angle of 164°. The H and C content, and O content of thinner films, was obtained using 16-30 MeV Si^{+5} Elastic Recoil Detection (ERD) at a scattering angle of 30°.

Hydration of the samples was performed by immersing the samples in de-aerated, distilled water for a period of 1560 minutes (26 hrs.). For samples used in electrical measurements, hydration was performed *prior* to deposition of the Au top contacts.

RESULTS AND DISCUSSION

Non-hydrated Oxides

The current-voltage measurements of the non-hydrated aluminum oxide films revealed the films to be highly insulating with an effective film resistivity over 5 x 10^{13} Ωcm (extrapolated from a linear fit to the low-bias region of the current-voltage plot), see Fig. 1. The current conduction process is non-ohmic, however, with a voltage dependence varying as $I \sim \exp(V^{\alpha})$. The current-voltage behavior is best described by a Frenkel-Poole conduction process, in which the current originates from thermal emission from defect traps within the oxide. At a given applied voltage, the magnitude of the leakage current is directly proportional to the trap density and exponentially proportional to the trap well depth. Therefore, the leakage current through the Al oxide layer may be used to assess the electronic defect concentration at the site of the electrical contact.

For higher applied fields, a different current conduction process through thin Al oxide layers may be operative. The extreme band gap of most alumina phases (about 7 eV) precludes direct carrier injection into the conduction band or valence band of the oxide, unless the oxide is thin enough and the field high enough. In this case, Fowler-Nordheim tunneling can occur. For a 100 Å thick aluminum oxide layer, it is estimated that direct Fowler-Nordheim tunneling will become significant above 3 to 4 V (this assumes that the band offset between metal Fermi level and oxide conduction band is approximately 2 to 3 eV). Therefore, near the point of dielectric breakdown, Fowler-Nordheim tunneling may become the dominant current conduction mechanism.

At applied electric fields higher than several MV/cm, dielectric breakdown of the Al oxide layer occurs. The dielectric breakdown event is characterized by an irreversible abrupt jump in film conductivity, typically by several orders of magnitude. The mechanism of dielectric breakdown (i.e. whether thermal-induced, hot carrier-induced, avalanche multiplication, etc.) in this material system is not presently known, but there is an asymmetry in the breakdown voltage depending on the polarization direction (whether the field between the Al and Au contacts is positive or negative). The magnitude of this asymmetry is aproximately 1 to 1.5 V, the breakdown voltage being higher for polarization in which the Au contact is at positive potential with respect to the Al contact (electron injection from the Al). This observation is consistent with the approximate 1 eV difference in work function between Au and Al, 5.3 eV and 4.3 eV, respectively (5), and the assumption that the dominant current transport mechanism at high field is Fowler-Nordheim emission.

The breakdown field of thin Al oxide layers is film thickness dependent, similar to what is commonly observed for other thin dielectrics, such as SiO_2 (6), see Fig. 2. This thickness dependence to the breakdown field is common in insulating systems, in which the breakdown mechanism is defect density dependent. At constant thickness, the magnitude of the breakdown field is an indication of the defect density of the oxide.

An example of the frequency-dependent electrical properties of a deposited Al oxide layer is shown in Fig. 3. The top panel, Fig. 3 (a), shows the frequency dependence of the oxide capacitance. The capacitance is almost independent of frequency, but shows a

slight downward slope which arises from the strong frequency dependence of the AC conductance, shown in Fig. 3 (b). Over most of this frequency range, the AC conductance is well-described by a dependence of the form, $G \propto \omega^{\alpha}$, with $\alpha = 1$. This observed frequency-dependent conductivity is very typical of many dielectric materials in which the current transport mechanism is defect-related, and the simplest explanation is that there exists within the sample a distribution of deep traps with different well depths, thus giving rise to a broad distribution of trap emission times (7). The magnitude of the AC conductance should be proportional to the defect density within the Al oxide layer.

From the sample geometry and observed capacitance, the dielectric constant of the Al oxide layer may be determined. This dielectric constant was determined to be about 9.5 for the deposited oxides, which is in good agreement with the range of accepted values for bulk alumina (corundum phase) of between 9 to 10 (8). For the ECR grown oxides, a lower average dielectric constant was observed, closer to 7. This lower value for the dielectric constant is consistent with the grown oxide layers being of lower density than the ECR deposited layers. X-ray reflectivity measurements indicated that the deposited oxide layers have a film density of 3.2 g/cm^3, while the ECR grown oxide layers have a density between 2.3 to 2.7 g/cm^3 – the densities of the corundum phase of Al_2O_3 is 3.97 g/cm^3 and the γ-phase is 3.5-3.9 g/cm^3 (5).

The above results suggest that solid state electrical measurements are suitable for assessing the electronic defect concentration within thin Al oxide layers on Al. For constant film thickness, an increase in electronic defect concentration would be manifested by a increase in DC leakage current, a reduction in breakdown field, and an increase in AC conductance. Using these electrical measurements, the change in defect concentration was measured for these non-hydrated Al oxides following a hydration treatment. These results are discussed below.

Hydrated Oxides

The hydrated oxides include ECR grown, ECR deposited, and synthetic air oxides which were all hydrated after deposition. The hydrated oxides also include the anodic oxides which were formed in an aqueous environment. Following hydration, very profound changes occurred in the electrical properties of the oxides as evidenced by Figs. 1 – 3. Hydration was found to greatly increase the leakage current of the oxides (Fig. 1), reduce the breakdown field (Fig. 2), and increase the dielectric constant of the films (Fig. 3 (a)). This trend was true for all of the hydrated samples, except the thicker anodic oxide samples.

X-ray reflectivity measurements revealed that changes occurred in the samples following hydration. The most significant change was that the ~ 200 Å thick ECR deposited oxides thinned slightly by approximately 10% (for the hydrated samples, this thickness is the total thickness inclusive of any surface aluminum oxy-hydroxide layer). Non-hydrated samples which were thinner than about 50 Å thickened slightly following hydration to about 50 Å. The air oxide also thickened to this value, suggesting that native oxide layers on Al will thicken to a limiting value of about 50 Å – at least for 26 hour immersion in room temperature water.

It is not surprising that water immersion can cause changes in thin Al oxide layers. The thermodynamically stable phase in the water – Al – oxygen system is gibbsite, $Al(OH)_3$. However, during immersion of Al in water, the first phase which is typically observed is pseudoboehmite, AlOOH (9). During later stages of hydration, bayerite [also $Al(OH)_3$] is observed. At elevated temperature in water, these hydroxide phases can grow to a thickness approaching 1 μm. The observed dielectric constant of the Al oxide films increases after hydration to 11 – 12, see Fig. 3 (a), which is consistent with the presence of at least a partial hydroxide layer on the Al oxide surface – the dielectric constant of boehmite is 20.5 (10).

What is surprising is the very large change in electrical conductivity of the Al oxide films, even for films which were formally excellent barrier layers, see Fig. 1. It is not believed that this large increase in electrical conductivity is due to water incorporation into the oxide layer since a vacuum de-hydration step was employed prior to electrical contact formation and SEM and TEM measurements of similar deposited Al oxide samples showed no porosity. Furthermore, no macroscopic defects (pits, etc.) were observed by SEM analysis of the ECR deposited oxide and grown oxide layers following hydration. If the electrical changes that occurred in the oxide layer were non-uniformly distributed, it would be necessary that these defect "sites" be distributed with a density much greater than 4×10^4 cm^{-2}, since all electrical contacts gave essentially the same results. Instead, it is believed that hydration leads to at least partial conversion of the barrier oxide layer to a hydroxide layer and significantly increases the electronic defect concentration within any remaining barrier layer which was not converted.

RBS and ERD analysis was performed on the Al oxide samples prior to and following hydration. The total O content of the oxide layers was found to be approximately constant following hydration, except for the 200 Å angstrom deposited oxide films, which showed a small reduction in O content – consistent with a slight thinning of the film as observed by x-ray reflectivity. More interestingly, the H content as measured by ERD of the films was observed to be significantly increased following hydration, and a significant tailing of the hydrogen into the Al metal layer is also observed, see Fig. 4. This "hydrogenation" suggests that hydration can promote hydrogen injection through the Al oxide layer. Unlike SiO_2 where H incorporation into the oxide can actually reduce the electronic defect concentration due to defect passivation, hydrogen in Al oxide may act as an electronic defect or as a defect-forming agent due to the ability of protons to disrupt bonding within the Al-O lattice.

As possible evidence of the role of hydrogen for electronic defect creation in hydrated Al oxide layers, the 100 Å thick anodic Al oxide sample – unlike all other hydrated samples – retained its insulating barrier layer properties despite being immersed in water. Anodic Al oxides are grown at anodic potentials (the Al metal being biased positive with respect to the counter electrode). With this field direction, protons should be expelled from the Al oxide layer, and this may be the reason for the apparent low electronic defect density of anodic Al oxides.

If hydrogen does promote electronic defect creation within hydrated Al oxide layers on Al, it may play a significant role for localized corrosion initiation. Sites in the Al oxide layer which are particularly susceptible to hydration will exhibit increased electronic defect concentration and reduced breakdown field and thus be susceptible to

passive layer electrochemical breakdown. These sites can be determined by solid state electrical measurement on samples with precisely defined or artificially-engineered electrochemically-active defects.

CONCLUSIONS

The electrical properties of native, anodic, and deposited Al oxide layers on Al were investigated prior to and following hydration. The DC leakage current, breakdown field, and AC conductance were found to be sensitive to the electronic defect concentration within the Al oxide film. Following hydration, the apparent electronic defect concentration greatly increased. Elastic recoil detection of hydrogen revealed a large increase in hydrogen concentration within the Al oxide layer and through the Al oxide layer. The increase in electronic defect concentration is related to the hydrogenation of the Al oxide film, and the effect of this hydrogenation may be an important mechanism for localized corrosion initiation.

ACKNOWLEDGMENTS

Valuable discussions with F. D. Wall, K. R. Zavadil, B. C. Bunker, H. S. Isaacs, and R. G. Buchheit are gratefully acknowledged. This work was supported by the U.S. DOE Office of Basic Energy Sciences, Metals and Ceramics Division. Sandia is a multiprogram laboratory operated by Sandia Corp., a Lockheed Martin Co., for the U.S. DOE under Contract DE-AC04-94AL85000.

REFERENCES

1. D. A. Jones, Principles and Prevention of Corrosion, Prentice Hall, Saddle River, NJ (1996).
2. L. F. Lin, C.-Y. Chao, and D. D. McDonald, J. Electrochem. Soc., 128, 1994 (1981).
3. M. M. Lohrengel, Mat. Sci. and Eng., R11, 243 (1993).
4. J. C. Barbour, D.M. Follstaedt, and S.M. Myers, Nucl. Instrum. Methods B, 106, 84 (1995).
5. CRC Handbook of Chemistry and Physics, CRC Press, Boca Raton, FL (1987).
6. E. Harari, J. Appl. Phys., 49, 2478 (1978).
7. S. R. Elliott, Physics of Amorphous Materials, John Wiley & Sons, New York (1990).
8. F. Singer and H. Thurnauer, Metallurgica, 36, 237 (1947).
9. R. S. Alwitt, J. Electrochem. Soc., 121, 1322 (1974).
10. O. Glemser, Z. Elektrochem., 45, 865 (1939).

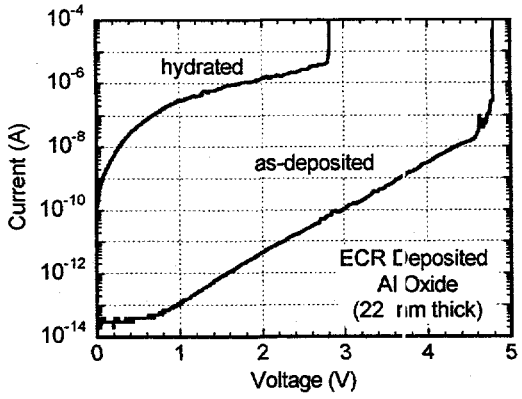

Fig. 1. Current-voltage characteristics for as-deposited and hydrated ECR deposited Al oxides on Al.

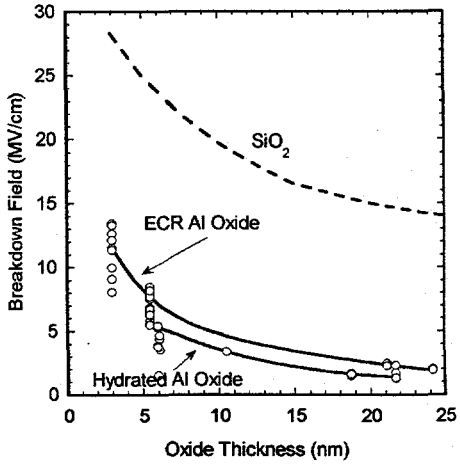

Fig. 2. Breakdown field as a function of oxide thickness for non-hydrated Al oxides and hydrated Al oxides. The thickness-dependence of the breakdown field of SiO_2 is shown for comparison (from Ref. 6).

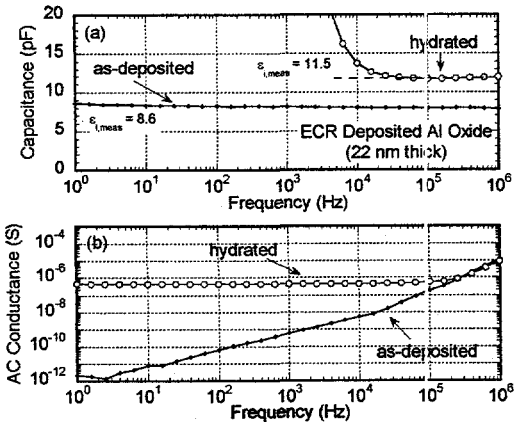

Fig. 3. (a) Capacitance and (b) AC conductance vs. frequency for an as-deposited and hydrated ECR deposited Al oxide on Al.

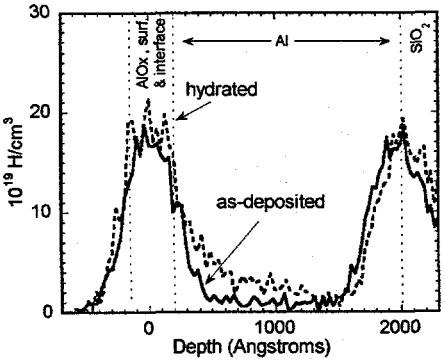

Fig. 4. H content for an as-deposited and hydrated ECR deposited Al oxide on Al as measured by ERD. The first peak includes H in the oxide and oxide surface and interface with the Al. The second peak is H at the Al/SiO_2 interface.